

STUDY OF DIRECTIONALLY SOLIDIFIED Fe – 4,25 %C EUTECTIC ALLOY USING ELECTRON BACKSCATTER DIFFRACTION (EBSD) TECHNIQUE

Received – Priljeno: 2019-11-19

Accepted – Prihvaćeno: 2020-03-10

Preliminary Note – Prethodno priopćenje

Electron back-scattered diffraction was used to determine the microstructure of a eutectic. Fe – 4,25 % C alloy was directionally solidified with the growth rate of 300 mm/h (83,3 $\mu\text{m/s}$) in a vacuum Bridgman-type furnace with liquid metal cooling. Eutectic phases have been observed using optical microscopy and scanning electron microscopy. The morphology of the eutectic phases was described. EBSD analysis reveals pronounced direction $\langle 100 \rangle$ of cementite in the microstructure produced by directional solidification.

Key words: Fe – eutectic, directional solidification; phase; EBSD; microstructure

INTRODUCTION

The conditions of solidification affect the properties of eutectics. Eutectics have a fine microstructure and are composite materials. The purpose of the eutectic studies is to determine their mechanical properties resulting from the reduction of interphase spacing, homogenization of the structure and the increase of interfaces surface. The Bridgman method allowed better understanding of the physical mechanisms controlling the microstructural development during directional solidification. The use of better techniques allows to understand the relationship between the properties and the microstructure of eutectics. This applies particularly to transmission electron microscopy, scanning electron microscopy, X-ray diffraction and electron back scatter diffraction techniques. The directional solidification conditions with a temperature gradient along with heat conduction direction also influence the growth of eutectic cementite.

Regarding eutectic growth, the structures are controlled by the ratio of the temperature gradient G to the growth rate v . A relatively high G/v value gives a quasi-regular lamellar structure with edgewise growth and a smaller G/v value results in a ledeburite structure with cooperation growth of austenite and Fe_3C . As there is no certainty how the growth texture of eutectic cementite is related to its growth morphology, this current study is aimed at investigating this relationship [1]. The studies of eutectic Fe - C alloys [2÷11] are well known. The subject of the increase in the ledeburitic eutectic was also discussed, defining the growth directions for cementite.

M. Trepczyńska-Łent, University of Science and Technology Bydgoszcz, Faculty of Mechanical Engineering, Poland, e-mail: małgorzata.trepczyńska-lent@utp.edu.pl

J. Piątkowski, Silesian University, Faculty of Materials Engineering and Metallurgy, Katowice, Poland

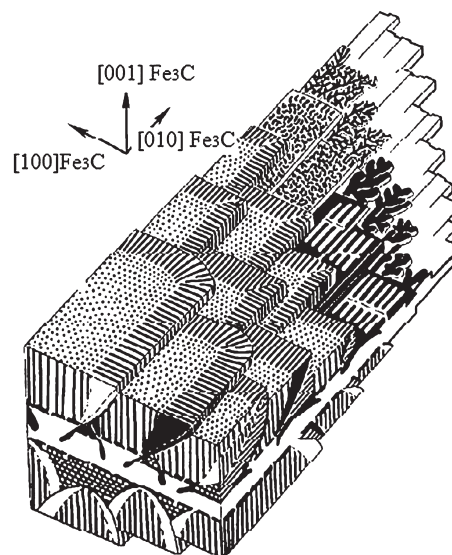


Figure 1 Three-dimensional model of $\text{Fe}(\gamma) - \text{Fe}_3\text{C}$ eutectic [2, 3, 5]

Figure 1 shows a 3-D model of $\text{Fe}(\gamma) - \text{Fe}_3\text{C}$ eutectic with directions: $\langle 010 \rangle$, $\langle 001 \rangle$, $\langle 100 \rangle$. Electron back scatter diffraction was used in the studies of directional solidification of Fe – C eutectic alloy. EBSD has a remarkable impact on the characterization of materials, including eutectics [8, 12÷14], through directly linking microstructure and crystallographic texture to provide quantitative data.

METHODOLOGY

Fe – 4,25% C eutectic alloy was prepared for this study in corundum crucible under the protection of argon gas in Balzers-type heater. Table 1 presents the chemical composition of this alloy.

The directional solidification was performed by the Bridgman method at the Faculty of Foundry Engineer-

Table 1 Chemical composition of Fe – 4,25 % C alloy / wt. %

C	Si	Mn	P	S	Cr	Ni	Mo	Al	Cu
4,25	0,057	0,64	0,0079	0,021	0,033	0,0093	<0,0020	0,011	0,032
Co	Ti	Ni	Nb	V	W	Pb	Mg	B	Sn
0,0024	<0,0010	0,0093	<0,0040	0,0022	<0,010	<0,0030	<0,0010	0,0009	0,0061
Zn	As	Bi	Ca	Ce	Zr	La	Fe		
<0,0020	0,0069	<0,0020	0,0005	<0,0030	0,0043	0,0013	94,9		

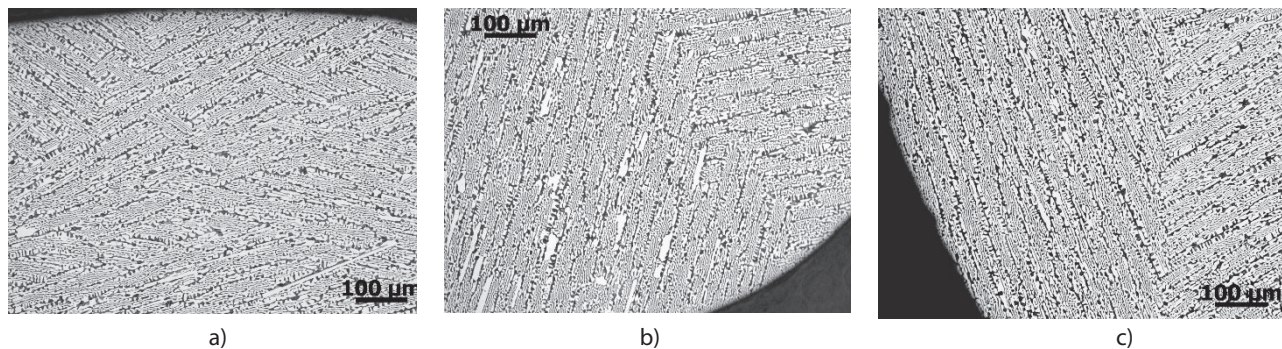


Figure 2 Transverse sections: a) area 1, b) area 2, c) area 3, LM, x 100, etched with Nital

ing, Department of Engineering of Cast Alloys and Composites at AGH in Krakow. The pulling process was performed at a growth rate of 300 mm/h (83,3 $\mu\text{m/s}$). The temperature gradient $G = 33,5 \text{ K/mm}$ was constant. Detailed information on the process is presented elsewhere [15, 16]. The sample of $\varnothing 5 \times 100 \text{ mm}$ was cut, ground and polished. The metallographic cross-sections were etched with 3 % Nital solution for light-optical microscopy Nikon MA100 equipped with Zeiss Erc5s digital camera and polished with Al_2O_3 suspension with a grain size of 0,05 μm for EBSD investigation, respectively. EBSD measurements aimed at and polished with Al_2O_3 suspension with a grain size of 0,05 μm for EBSD investigation, respectively. EBSD measurements aimed at determining the presence of microstructure by measuring the directional topography, the pole figures, the inverse pole figures and phase composition maps for the sample of the metastable eutectic alloy after directional solidification, with the pulling rate being 300 mm/h. Electron back-scattered diffraction, which can monitor concurrent particles individually and correlate the results to the microstructure, was adopted in this study. The microstructure of the eutectic was examined using an EBSD system interfaced to a Hitachi S–3400N. The measurements were performed at Institute of Materials Science, Faculty of Materials Engineering and Metallurgy at Silesian University of Technology. EBSD measurements were conducted using a Carl Zeiss LEO 1530 field emission scanning electron microscope (SEM) equipped with the detector INCA HKL Nordlys II Channel 5 system. Acceleration voltage was set to 20 kV using a magnification of 1 000 x and a step of electron beam travel equal to 0,5 μm . The study was performed in three different areas on the transverse section of the sample (hereinafter referred to as: area 1, area 2, area 3).

RESULTS AND DISCUSSION

The microstructure on the transverse sections of Fe – 4,25 % C eutectic alloy is shown in Figures 2 a, b, c) for area 1, area 2, area 3, respectively. The microstructure is composed of austenite dendrites (largely decomposed to fine pearlite) embedded in a eutectic matrix: plate-like cementite – bright and pearlite – dark. The matrix of cementite eutectic in Fe – 4,25 % C appears to be continuous.

Figure 3 a shows the phase composition map obtained in the transverse section of the crystallized rod of the Fe – 4,25 % C eutectic alloy (the direction of solidification has been perpendicular to the map plane). The cementite section was marked in blue, whilst the iron one – in red. The map of the crystallographic orientation of this section was shown in the Figure 3 b.

The colour scheme of the inverse Z pole figure was used, which has enabled easy interpretation of the map: the particular colours in the map relate to the stereographic triangles corresponding to every phase (Fe and Fe_3C). The comparison between the orientation map and the phase composition map reveals that the cementite orientation is similar to the $\langle 100 \rangle$ orientation (blue colour in the orientation map) – which means that the $\langle 100 \rangle$ direction of cementite is nearly parallel to the direction of solidification.

For example, for area 1, the pole figures are shown to confirm observation for cementite in Figure 4.

The experimentally determined pole figures are very similar to the theoretical figures for the orthorhombic crystal system. The highest pole densities for the pole figure $\{100\}$ are located very close to the centre of the figure, which translates into a slight angle deviation between the $\langle 100 \rangle$ cementite direction and the direction of solidification. The highest pole densities in the $\{010\}$ and $\{001\}$ figures are shifted in relation to the ideal po-

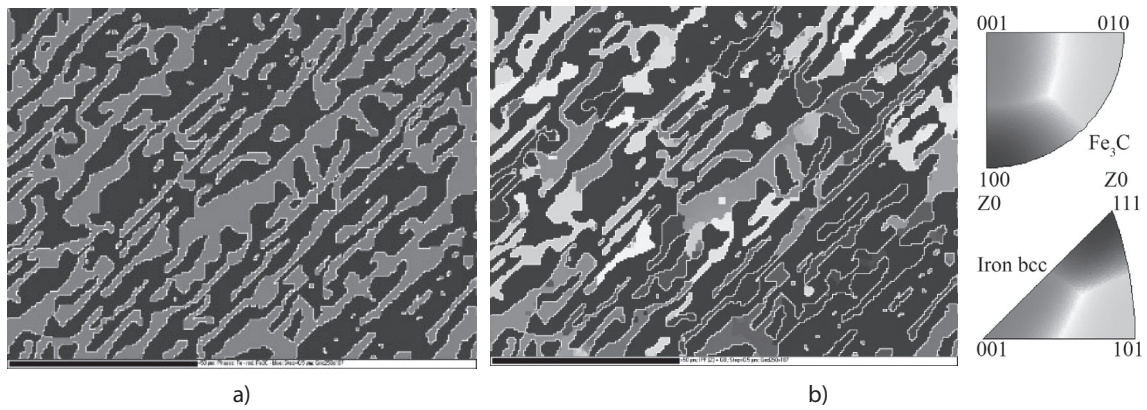


Figure 3 (a) Phase composition map: black – Fe₃C, grey – Fe, (b) crystallo-graphic orientation map (IPF colour scheme)

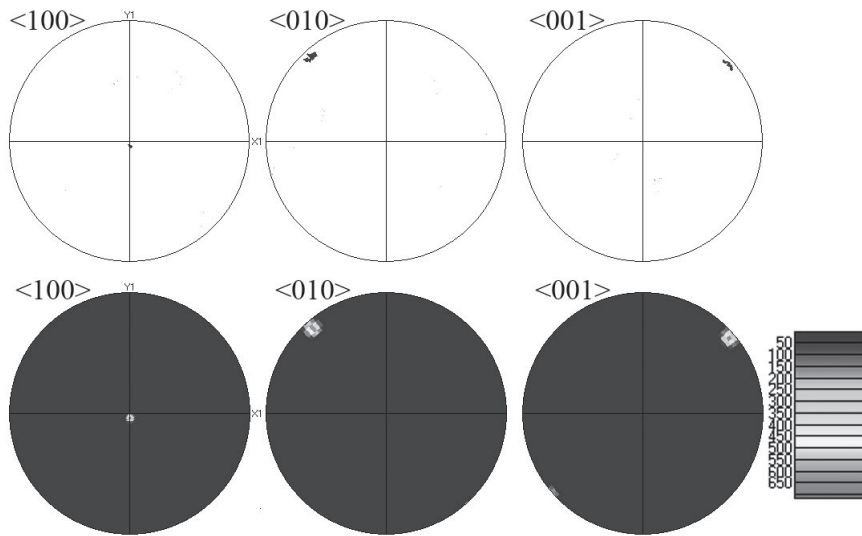


Figure 4 Pole figures of cementite – area 1

sitions, which is merely a sign of the rotation of the crystal structure of cementite around the $\langle 100 \rangle$ direction. Moreover, on each figure $\{010\}$ and $\{001\}$ there is only one visible highest pole density – it is related to the angle deviation of the $\langle 100 \rangle$ direction from the direction of solidification, which makes the opposite highest pole density shifted off the periphery of the directional figure. The inverse pole figures confirm the information gained with the pole figures: the slight angle deviation between the $\langle 100 \rangle$ direction and the direction of solidification and the rotation of the crystal structure of cementite around the $\langle 100 \rangle$ direction.

In the analysed area 1, the 3,7 % of cementite grains were characterized by a deviation in the range of $3 \div 4^\circ$, the 65,9 % of grains in the range of $4 \div 5^\circ$ and the 30,1 % of grains - in the range of $5 \div 6^\circ$. The average value of the angle deviation of cementite direction $\langle 100 \rangle$ from the crystallization direction, determined on the basis of the measurements, is $4,75^\circ$. The orientation of the directionally solidified sample is complemented by the distribution of the orientation, quantifying the relative incidence of a specific angular deflection of direction $\langle 100 \rangle$ from the direction of solidification.

In area 2, most cementite grains are characterised by the deviation of the $\langle 100 \rangle$ direction from the direction

of solidification by $1 \div 2^\circ$ and $3 \div 4^\circ$. The average value of the angle deviation of the $\langle 100 \rangle$ direction from the direction of solidification is $1,98^\circ$.

For area 3, the distribution of cementite orientation captures these observations in a strictly quantitative manner – there is a lack of grains characterized by angle deviation in the range of $5 \div 6^\circ$. The average value of the angle deviation of the direction $\langle 100 \rangle$ from the solidification direction is 4,2 – in this case.

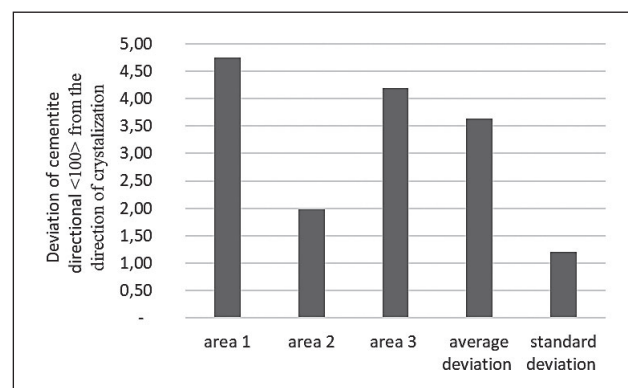


Figure 5 Angle deviation of direction $\langle 100 \rangle$ from the crystallization direction of cementite

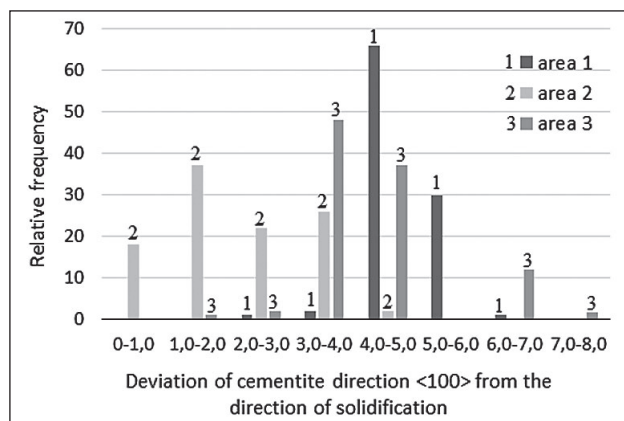


Figure 6 Distribution of the orientation of cementite

The average value of the angle deviation determined from measurements on three areas is $3,64^\circ$ (Fig. 5). The distribution of cementite orientation for all studied areas is shown in Figure 6. The deviation of cementite direction $\langle 100 \rangle$ from the direction of solidification ranges from 0 to 8.

SUMMARY

The studied Fe – 4,25 % C eutectic alloy was directionally solidified. An analysis of the crystallographic orientation made with the EBSD technique showed that for the studied cementite, a plate-like microstructure $\langle 100 \rangle$ was observed. Direction $\langle 100 \rangle$ is slightly deviated from the direction of crystallization. The average value of this angle deviation determined from measurements in three areas is $3,64^\circ$. For the studied iron, Fe(α), there was no strong trend towards directional solidification – only in area 3 slight fibrous microstructure $\langle 100 \rangle$ can be seen.

A strong preferred $\langle 100 \rangle$ growth direction exists for the cementite. On the other hand, the Fe(α), with irregular appearance has a diffused structure.

This study suggests that the growth direction of the eutectic cementite is dependent on heat transfer during solidification. Curved eutectic cementite and plate-like cementite with straight interfaces clearly differ from each other on microstructural level. In the plate-like cementite strong preferred $\langle 100 \rangle$ growth direction occurs. Known in the literature, the leading direction of the growth of the cementite phase $\langle 100 \rangle$ and the growth direction $\langle 100 \rangle$ of cementite coincides in this work with the radius of the rod sample.

Acknowledgements

The author wishes to express gratitude to Prof. E. Guzik, PhD E. Olejnik and PhD A. Janas from Faculty of Foundry Engineering, Department of Engineering of Cast Alloys and Composites at AGH University of Science and Technology in Krakow.

REFERENCES

- [1] J.Z. Li, M. Kaya, R.W. Smith, *Journal of Crystal Growth* 133 (1993), 175-180
DOI: 10.1016/0022-0248(93)90118-G
- [2] K.P. Bunin., I.N. Malinotchka, I.N. Taran, *Osnovi Tchuguna, Metallurgyia, Moscow*, 1969
- [3] Ju.N. Taran, V.I. Mazur, *Struktura Ėvtekticheskikh Splavov, Metallurgiya, Moskwa*, 1978
- [4] P. Magnin, R. Trivedi, *Acta Metallurgica et Materialia* 39 (1991), 453-467.
DOI: 10.1016/0956-7151(91)90114-G
- [5] V. Mazur, A. Mazur, *Novi materialy i tekhnolohiyi v metalurhiyi ta mashynobuduvanni 1* (2011), 17-26
- [6] H. Jones, W. Kurz, *Zeitschrift für Metallkunde* 72 (1981), 792-797
- [7] J. S. Park, J. D. Verhoeven, *Metallurgical and Materials Transactions A* 27A (1996), 2328-2337 DOI: 10.1007/BF02651887
- [8] J.M. Song, L. Chen, T. Lui, *Materials Science and Engineering A* 347 (2003), 5-8, DOI: 10.1016/S0921-5093(02)00177-6
- [9] W. Wolczyński, *Crystal Research and Technology* 27 (1992), 121-125, DOI: 10.1002/crat.2170270122
- [10] E. Guzik, D. Kopyciński, *Metallurgical and Materials Transactions A* 37 (2006), 3057-3067, DOI: 10.1007/s11661-006-0187-7
- [11] A. Leineweber, S.L. Shang, Z.K. Liu, *Acta Materialia* 86 (2015), 374-384,
DOI: 10.1016/j.actamat.2014.11.046
- [12] S. Kante, A. Leineweber, *Materials Characterization* 138 (2018), 274-283
DOI: 10.1016/j.matchar.2018.01.032
- [13] A.J. Wilkinson, T.B. Britton, *Materials Today* 15 (2012), 366-376,
DOI: 10.1016/S1369-7021(12)70163-3
- [14] D. Siekaniec, D. Kopyciński, *Journal of Casting & Materials Engineering* 1 (2017), 15-19
DOI: 10.7494/jcme.2017.1.1.15
- [15] M. Trepczyńska-Łent, *Archives of Metallurgy and Materials* 58(3) (2013), 987-991, DOI: 10.2478/amm-2013-0116. DOI: 10.2478/amm-2013-0116
- [16] M. Trepczyńska-Łent, *Crystal Research and Technology* 52(8) (2017), DOI: 10.1002/crat.201600359.

Note: The responsible for English language is Aleksandra Pawlicka; Bydgoszcz, Poland